

## CHAPTER IV

### RESULTS AND DISCUSSION

This chapter illustrates and discusses about the catalyst characterization and catalytic activity results of unmodified and modified HZSM-5 with various amounts of metallic Ni and Mo. The morphological textural and chemical properties of catalysts were studied by means of XRD, XRF, SEM, Surface area analysis, H<sub>2</sub>-TRR, TPO, and TPD-IPA. Moreover, the relation of catalyst properties and catalytic activity was explained in more detail to understand the effect of catalyst on methane dehydrogenation and coupling reaction.

#### 4.1 Catalyst Characterization

The HZSM-5 commercial catalyst and HZSM-5 incorporated with various amounts of Ni and Mo metal were studied to understand the characteristic of catalysts related to the catalytic performance in methane conversion. According to this purpose, the catalyst composition, morphology, surface area, pore volume, reducibility as well as acidity were investigated by various techniques which were described below.

##### 4.1.1 X-ray Diffraction (XRD)

The catalyst structure and particle size of NiO and MoO<sub>3</sub> were investigated by XRD technique. The scanning region of the diffraction angle  $2\theta$  was 5 to 80°, which covers most of the significant diffraction peaks of the zeolite. The XRD patterns of the parent HZSM-5 with molar Si/Al ratio of 25 and the bimetallic Ni-Mo/HZSM-5 with different Ni loading at 0.5 wt% to 3 wt% and Mo loading at 3 wt% are presented in Figure 4.1. The similarity of the XRD patterns between the parent HZSM-5 and the modified HZSM-5 indicates that the framework of HZSM-5 was still retained during polyol mediated process. By comparing with the HZSM-5 pattern, modified HZSM-5 with 3%Ni showed similarity of peak intensity indicating that NiO dispersed on the external surface of HZSM-5. The peak intensity of HZSM-5 decreased at the 3%Mo loading on HZSM-5. This can imply that the some

portion of  $\text{MoO}_3$  entered into the channels of HZSM-5. Moreover, the intensities of peak of modified HZSM-5 with Ni and Mo decreased as the Ni loading increased. The decreased of peak intensity of bimetallic catalyst implied the entrance of NiO and  $\text{MoO}_3$  into channels of HZSM-5 (Li *et al.*, 2006). The addition of Mo could help the NiO disperse into the HZSM-5. The crystalline phases of NiO and  $\text{MoO}_3$  could not be observed in the XRD patterns. This may indicate that the nickel and molybdenum species were finely dispersed on the external surface or located in the channels of the HZSM-5 zeolite with a small amount of metals ( $< 5 \text{ wt}\%$ ) (Chen *et al.*, 1995).

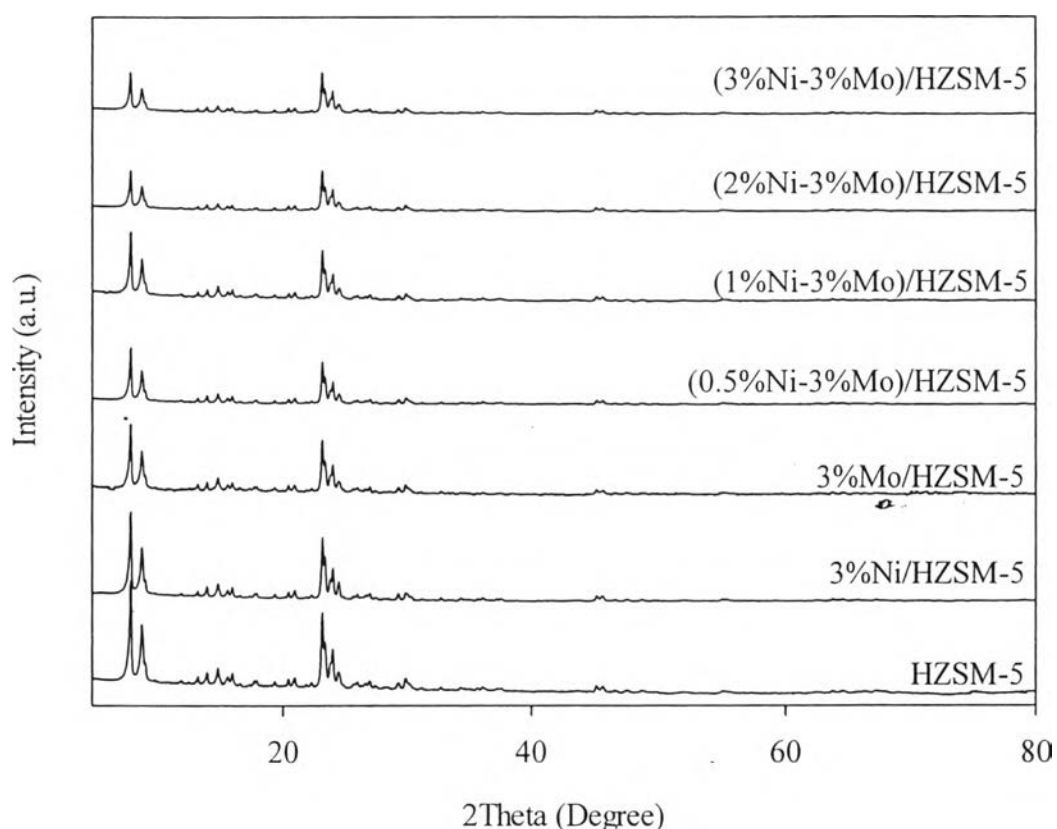


**Figure 4.1** The XRD patterns of parent HZSM-5 and modified HZSM-5.

The metal ion promoted on HZSM-5 zeolite has been found to be effective in the transformation of methane to ethylene. Phase analysis by XRD technique demonstrated that only a HZSM-5 phase was observed when the metal

loading was low. However, the crystalline size of NiO and MoO<sub>3</sub> was calculated from the data that obtained by XRD technique. The average crystalline size of NiO and MoO<sub>3</sub> prepared by polyol mediated method are shown in Table 4.1. It can be observed the crystalline size of NiO in 3%Ni/HZSM-5 was larger than MoO<sub>3</sub> in 3%Mo/HZSM-5. Moreover, the crystalline size of NiO on the bimetallic catalyst decreased comparing with 3%Ni/HZSM-5. The cooperation between Ni and Mo on HZSM-5 could help to be the small crystalline size of NiO. Moreover, the average particle sizes of NiO and MoO<sub>3</sub> are smaller than the Ni-Mo/ZSM-5 catalyst prepared by impregnation method as referred to the literature (Vosmerikov *et al.*, 2009). Furthermore, the crystalline size of alloy Ni and Mo indicated in NiMoO<sub>4</sub> implied that the crystalline particle size of NiMoO<sub>4</sub> tended to increase with increasing Ni loading.

**Table 4.1** The crystalline size which formed on the different catalyst

Catalyst	NiO Size (nm)	MoO <sub>3</sub> Size (nm)	NiMoO <sub>4</sub> Size (nm)
3%Mo/HZSM-5	-	37.08	-
3%Ni/HZSM-5	42.74	-	-
(0.5%Ni - 3%Mo)/HZSM-5	33.58	40.48	29.17
(1%Ni - 3%Mo)/HZSM-5	37.82	39.35	29.91
(2%Ni - 3%Mo)/HZSM-5	36.32	40.40	31.31
(3%Ni - 3%Mo)/HZSM-5	36.48	41.56	33.77

#### 4.1.2 X-ray Fluorescence (XRF) Analysis

XRF technique was employed to identify the Si/Al ratio and the amount of Ni and Mo loading which would effect on the dehydrogenation and coupling reaction. The Si/Al molar ratios and chemical compositions of catalyst are presented in Table 4.2. It is observed that the Si/Al ratio of HZSM-5 zeolite does not significantly change while the amount of Ni and Mo loading was incorporated

implying that the addition of metal particles does not affect to the Si/Al ratio of HZSM-5 zeolite. The fraction of Ni and Mo that show the small value ( $< 5$  wt%) indicated the small amounts of metal particle addition. It can support the crystalline phases of metal were not detected in the XRD result due to small amounts of loading. Moreover, the mass fractions of Ni and Mo are lower than the designed weight which may due to the reason that catalysts cannot be avoided absorbing water in the air before XRF analysis (Li *et al.*, 2011).

**Table 4.2** Chemical compositions of the prepared catalysts

Catalyst	Chemical Composition				
	Si (wt%)	Al (wt%)	Ni (wt%)	Mo (wt%)	Si/Al molar ratio
HZSM-5	95.93	4.07	-	-	22.72
3%Ni/HZSM-5	92.99	4.15	2.86	-	21.63
3%Mo/HZSM-5	93.43	4.01	-	2.56	22.47
0.5%Ni-3%Mo/HZSM-5	92.96	4.06	0.45	2.53	22.10
1%Ni-3%Mo/HZSM-5	92.33	4.09	0.92	2.66	21.40
2%Ni-3%Mo/HZSM-5	92.20	3.94	1.54	2.32	22.50
3%Ni-3%Mo/HZSM-5	90.72	3.89	2.64	2.75	22.45

#### 4.1.3 Field Emission Scanning Electron Microscopy (FE-SEM)

SEM was employed to observe the morphology of catalyst. The changing morphology of unmodified HZSM-5 compared to 2%Ni-3%Mo/HZSM-5 catalyst before reaction testing is presented in Figure 4.2 and 4.3. The morphology of unmodified HZSM-5 and 2%Ni-3%Mo/HZSM-5 shows the same morphology of small shape. It can observe that the morphology of the unmodified HZSM-5 was not changed when modified with 2 %Ni and 3 %Mo. From Table 2.7, 2%Ni-3%Mo/HZSM-5 catalysts provided the highest of coke formation at the same reaction conditions. It was easy to observe the changing of morphology after reaction testing. The morphological images of 2%Ni-3%Mo/HZSM-5 after the reaction testing at different temperatures of 750 °C and 800 °C are illustrated in Figure 4.4 and 4.5,

respectively. The some structure of spent catalyst slightly changed and the coke formation was observed at reaction temperature 750 °C and 800 °C.

The element mapping of 2%Ni-3%Mo/HZSM-5 catalyst by FE-SEM is shown in Figure 4.6. The contribution of the elements Ni, Mo, Si and Al is homogeneous and highly dispersed on the surface of catalyst (Li *et al.*, 2006).

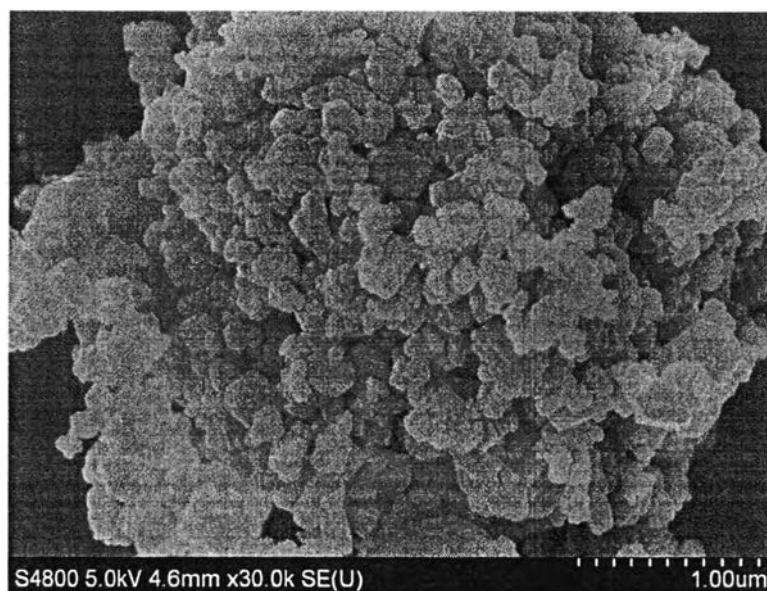


**Figure 4.2** SEM images of parent HZSM-5.

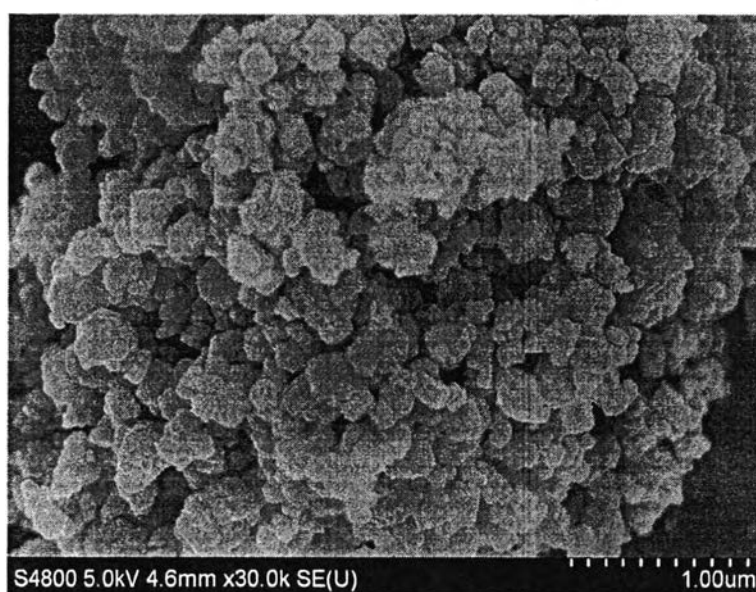


**Figure 4.3** SEM image of fresh 2%Ni-3%Mo /HZSM-5.

I 28368496

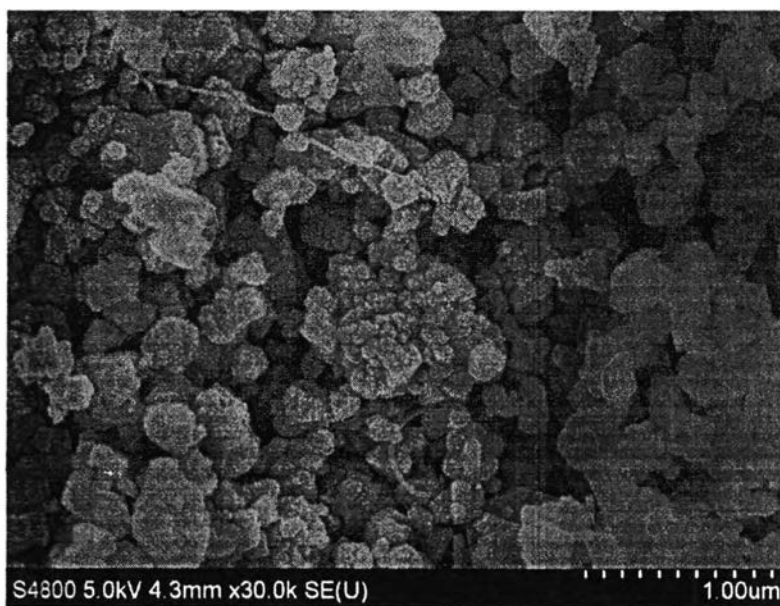


**Figure 4.4** SEM image of spent 2%Ni-3%Mo/HZSM-5 at reaction temperature 750 °C.

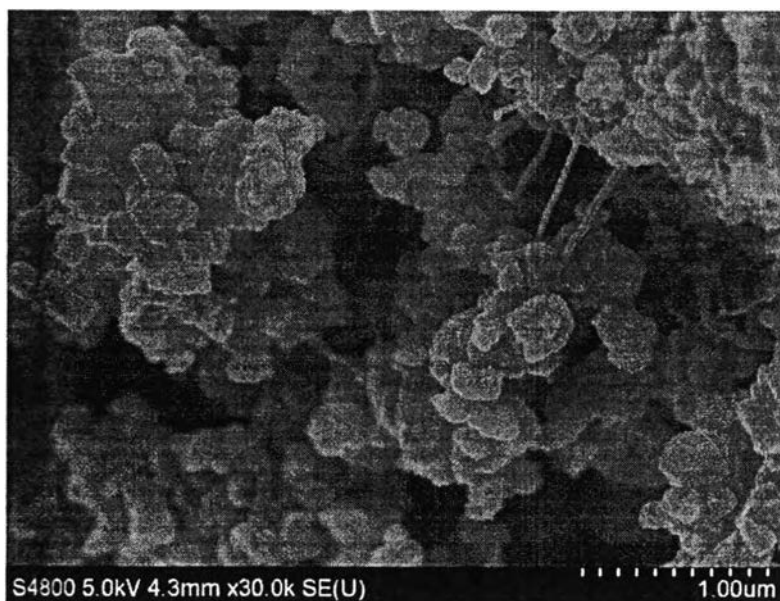


**Figure 4.5** SEM image of spent 2%Ni-3%Mo/HZSM-5 at reaction temperature 800 °C.

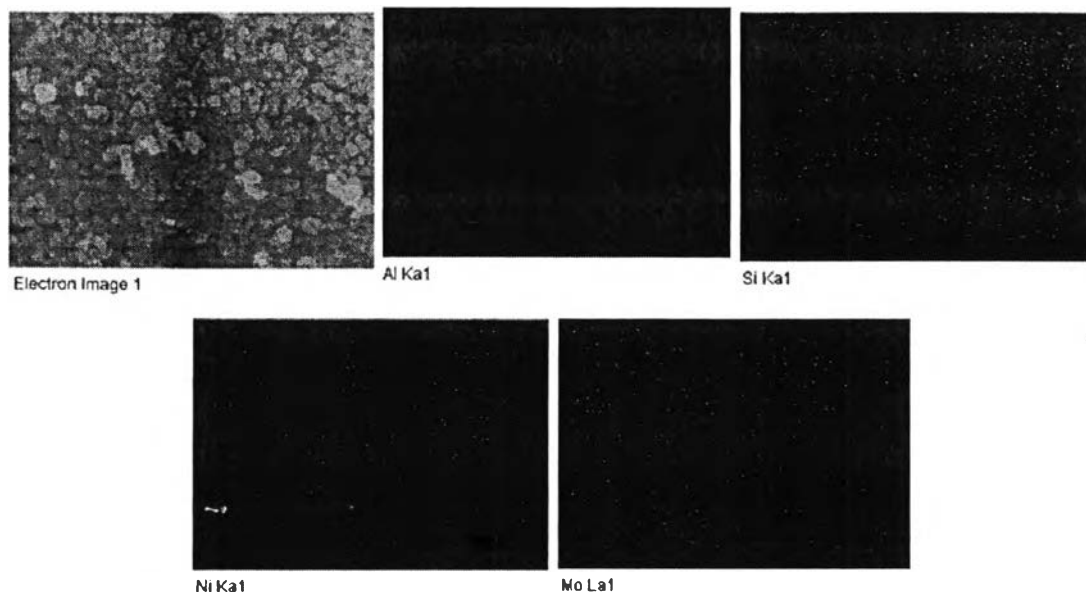


**Figure 4.6** Element mapping of the 2%Ni-3%Mo/HZSM-5 catalyst.

#### 4.1.4 Determination of Textural Properties

The textural properties of catalysts were determined by N<sub>2</sub> adsorption-desorption technique with the BET method. The BET surface area of various catalysts is summarized in Table 4.3. BET surface area of parent HZSM-5 decreased when monometallic 3 %Ni and 3 %Mo were introduced onto the zeolite. The surface area of 3%Mo/HZSM-5 (342 m<sup>2</sup>/g) was slightly higher than that of 3%Ni/HZSM-5 (322 m<sup>2</sup>/g). This result probably affected of the formation of Mo species clusters on the external surface. Both BET surface areas and micropore volumes of the modified HZSM-5 catalysts are decreased compared with those of the parent HZSM-5. Moreover, the surface area and micropore volume are decreased with increasing Ni loading as compared to the 3%Mo/HZSM-5 catalyst. This can be explained that some portions of metal loading would be dispersed on the surface (Li *et al.*, 2006) and another portion would enter into the channels of HZSM-5 zeolite causing the pore blocking (Chen *et al.*, 1995). In case of total pore volume, most of the modified HZSM-5 catalysts exhibit higher total pore volume than the parent HZSM-5. It is probably of the formation of small metal clusters on the external surface generating additional mesopores.

**Table 4.3** Textural properties of the catalysts studied

Catalyst	BET Surface Area (m <sup>2</sup> /g)	Total Pore Volume (cm <sup>3</sup> /g)	Micropore Volume* (cm <sup>3</sup> /g)
HZSM-5	385	0.458	0.121
3%Ni/HZSM-5	322	0.536	0.106
3%Mo/HZSM-5	342	0.523	0.116
0.5%Ni-3%Mo/HZSM-5	339	0.508	0.118
1%Ni-3%Mo/HZSM-5	300	0.447	0.101
2%Ni-3%Mo/HZSM-5	304	0.511	0.106
3%Ni-3%Mo/HZSM-5	280	0.455	0.093

\*Using t-plot method

#### 4.1.5 Temperature Programmed of Reduction (TPR)

Temperature programmed reduction (TPR) technique was carried out to investigate the reducibility of the Ni–Mo/HZSM-5 catalysts. The TPR profiles of all prepared catalysts are shown in Figure 4.7. For the parent HZSM-5, no peak of H<sub>2</sub> consumption was observed due to the absence of metal species. For modified HZSM-5 with Ni and Mo loading, a broad peak of hydrogen consumption between 400-700 °C can be observed. This evidence confirms the presence of NiO and MoO<sub>3</sub> in HZSM-5 support despite not detected by XRD. The TPR profiles with the Ni loadings have two broad peak, indicating that the metallic located on two different sites of HZSM-5. The first peak at low temperature (between 400 and 700 °C) is most probably the peak for the presence of metallic outside the external surface of HZSM-5 while the high temperature peak (> 700 °C) is due to the presence of dispersed metallic species inside the mesopore of HZSM-5 (Sarkar *et al.*, 2012). Furthermore, the amount of H<sub>2</sub> consumption depends on the amount of metal loading supported on the catalyst. Therefore, 3%Ni-3%Mo/HZSM-5 illustrates the highest H<sub>2</sub> consumption among those of modified HZSM-5 catalysts.



The metal dispersion is another important parameter related to the nature of catalyst. In particular, the metal active sites showed the important role in the dehydrogenation and coupling reaction that used the metal sites to converted methane into olefins. The high metal dispersion provided the high catalytic activity. The metal dispersion of various catalysts is summarized in Table 4.4. It can be observed that increasing of metal on HZSM-5 resulted in the decreased metal dispersion. This evidence supported the crystalline size that was investigated by XRD technique. The low metal dispersion indicated the large particle formation on the surface due to the agglomeration of particle.

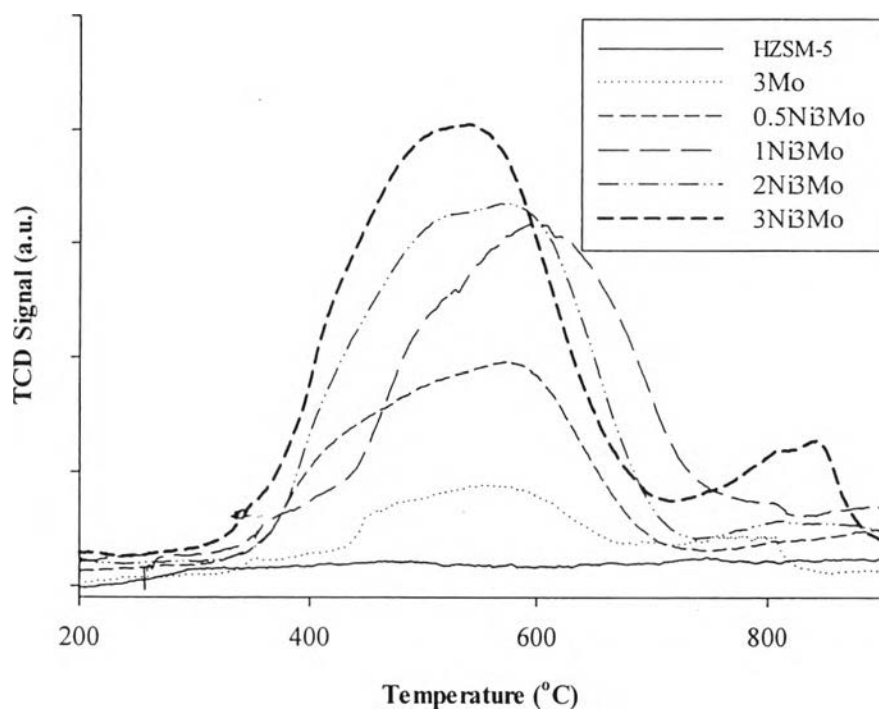


**Figure 4.7** TPR profiles of the prepared catalysts.

**Table 4.4** Metal dispersion of all loaded catalysts

Catalyst	Metal Dispersion (%)
3%Ni/HZSM-5	4.44
3%Mo/HZSM-5	4.72
0.5%Ni-3%Mo/HZSM-5	4.88
1%Ni-3%Mo/HZSM-5	4.34
2%Ni-3%Mo/HZSM-5	3.96
3%Ni-3%Mo/HZSM-5	2.89

#### 4.1.6 Temperature Programmed Desorption of Isopropylamine (IPA-TPD)

The acidity of catalysts is an important role because the methane dehydrogenation and aromatization reactions take place on these acid sites especially, Brönsted acid sites. The IPA-TPD profile of all catalysts are shown in Figure 4.8 exhibiting the amounts of Brönsted acid sites of unmodified HZSM-5 and modified HZSM-5. It indicates that unmodified HZSM-5 has a larger number of the Brönsted acid sites than the modified HZSM-5. The number of Brönsted acid sites of various catalysts is summarized in Table 4.5. It can be seen that the Brönsted acid sites was decreased with increasing Ni loading on Mo/HZSM-5. This can be suggested that the Brönsted acid sites were partially covered by Ni and Mo particles which restricted the Brönsted acid sites to interact with IPA. This result can support by the decreasing of the total pore volume that was investigated by surface area analysis because some Ni and Mo entered into the microporous or block the channels of HZSM-5 zeolite. Similar are the explanations on the decreased surface areas and total pore volume as given in section.

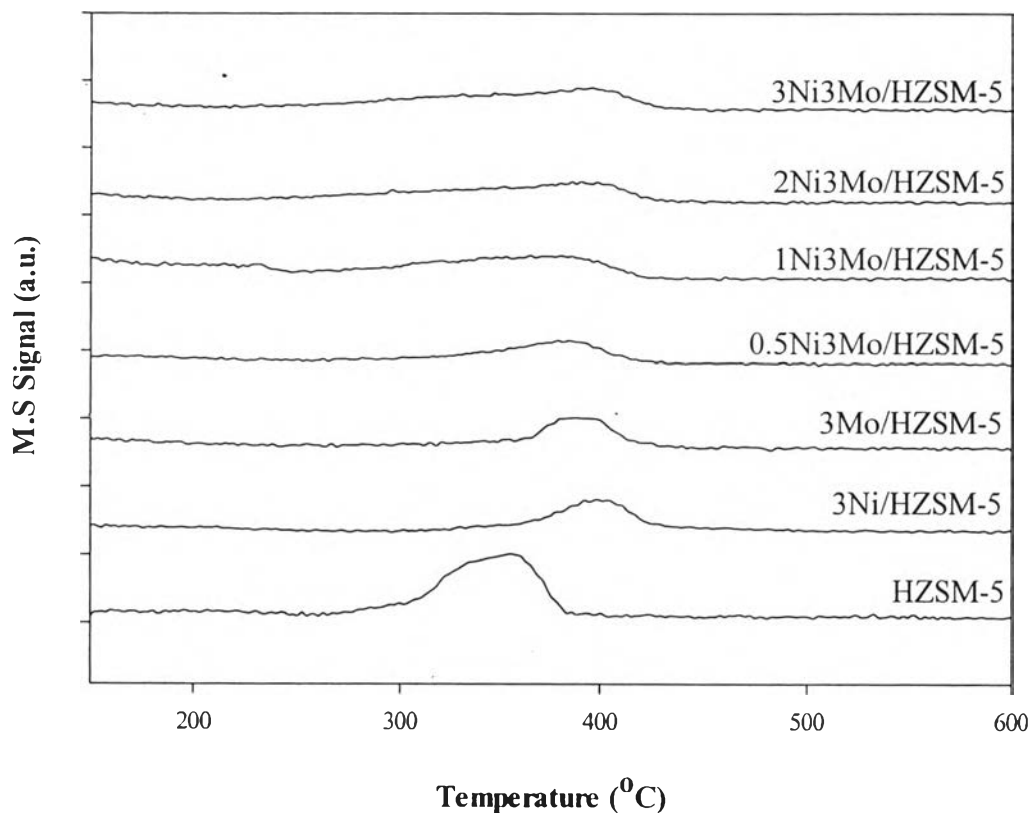


**Figure 4.8** IPA-TPD profiles of parent HZSM-5 and modified HZSM-5 catalysts.

**Table 4.5** The amount of the Brönsted acid sites of the catalysts investigated

Catalyst	Brönsted Acid Site ( $\mu\text{mol/g}$ )
HZSM-5	474
3%Ni/HZSM-5	287
3%Mo/HZSM-5	279
0.5%Ni-3%Mo/HZSM-5	348
1%Ni-3%Mo/HZSM-5	312
2%Ni-3%Mo/HZSM-5	271
3%Ni-3%Mo/HZSM-5	257

## 4.2 Catalytic Activity Testing for Non-Oxidative Methane Conversion

To study the performance of all prepared catalysts for methane dehydrogenation and coupling reaction, the catalysts were tested for their catalytic activity under various conditions to obtain methane conversion and selectivity to ethylene. With this regard, the effects of Ni and Mo loading, reaction temperature, methane feed concentration were investigated and discussed in the following sections.

### 4.2.1 Effect of Ni Loading

The metal site plays the important role that responsible for converts methane into olefins. The effect of Ni and Mo loading incorporated into HZSM-5 was tested for the reaction using a continuous down flow fixed-bed reactor under non-oxidative conditions at atmospheric pressure, GHSV of 1,500 ml/g/h. The catalytic performances of the catalysts studied shown in Figures 4.9 and 4.10.

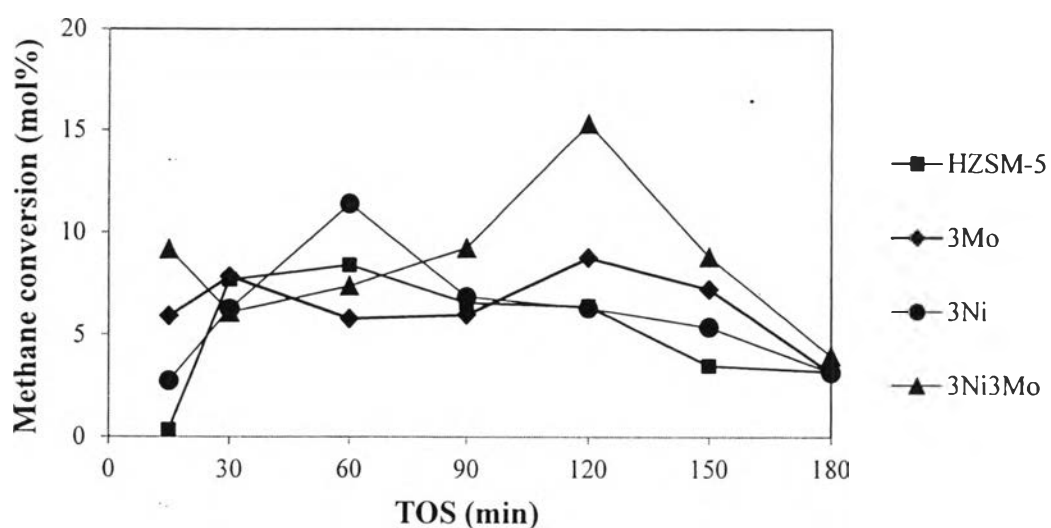


**Figure 4.9** Methane conversion over HZSM-5, 3%Ni/HZSM-5, 3%Ni/HZSM-5, and 3%Ni-3%Mo/HZSM-5 (750 °C, 20 % CH<sub>4</sub> balanced in N<sub>2</sub>, GHSV = 1,500 ml/g/h)

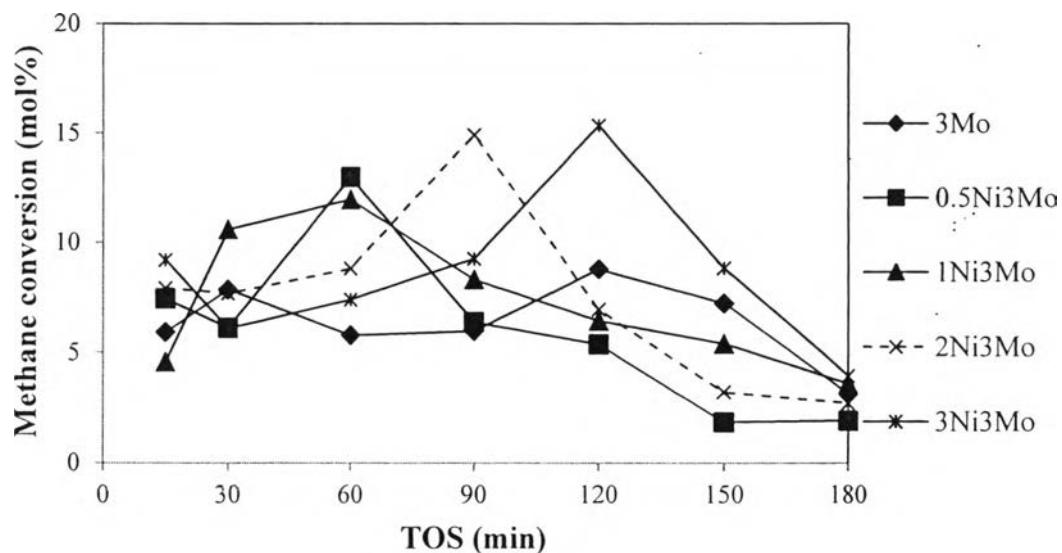


**Figure 4.10** Methane conversion over different Ni loading on 3%Mo/HZSM-5 (750 °C, 20% CH<sub>4</sub> balanced in N<sub>2</sub>, GHSV = 1,500 ml/g/h)

From Figure 4.9, unmodified HZSM-5 has the methane conversion lower than modified HZSM-5. The monometallic 3%Ni/HZSM-5 and 3%Mo/HZSM-5 catalysts provided the methane conversion lower than bimetallic ones. From Figure 4.10, the catalysts modified with 0.5 to 3 wt% Ni loading give higher overall methane conversion than the 3%Mo/HZSM-5 catalyst. However, a maximum methane conversion of the catalysts was reached at a different period of TOS by which a more content of Ni could prolong its maximum conversion. The 3%Ni-3%Mo/HZSM-5 catalyst provides the highest more activity, the maximum methane conversion is 15.34 % and rapidly decreased after TOS = 120 min due to coke deposit on catalyst. This can be suggested that the addition of Ni not only pronounced the activity, but also generated coke which in turn covered the active sites resulting in the poor catalytic activity eventually (Aboul-Gheit *et al.*, 2012).

In terms of products selectivity, Figure 4.11 shows the selectivity of gaseous products including ethylene, benzene, and toluene. The unmodified HZSM-5 cannot detect the gaseous product selectivity. In case of monometallic incorporation, the 3%Ni/HZSM-5 catalyst gives a constant ethylene selectivity of 100 % meanwhile the 3%Mo/HZSM-5 provides both ethylene and aromatics

selectivity. In case of bimetallic catalyst, the incorporation of Ni onto 3%Mo/HZSM-5 resulted in enhancing the ethylene selectivity. The 3%Ni-3%Mo/HZSM-5 catalyst provides the highest selectivity to ethylene of over 90 % and the lowest selectivity to aromatics of less than 10 % at any given TOS.

From the bifunctional catalyst behavior, the metal sites and Brönsted acid sites of zeolite played important roles in the conversion of methane into olefins and aromatics (Shu *et al.*, 1999). It is suggested that high ethylene selectivity on bimetallic catalyst was probably due to the low amount of Brönsted acid sites as shown in Table 4.5. The incorporation of Ni can cause the Brönsted acid sites to decline due to the partial pore blockage. The 3%Ni-3%Mo/HZSM-5 provides the lowest Brönsted acid sites which are responsible for the aromatization reaction. When the Brönsted acid sites were deactivated by coke formation, therefore ethylene formed on the metal sites would be converted into aromatics in low amounts, thus decreasing the aromatics selectivity. It can be indicated that Ni would play a significant role in enhancing the formation of ethylene and at the same time suppressing the aromatization of ethylene.

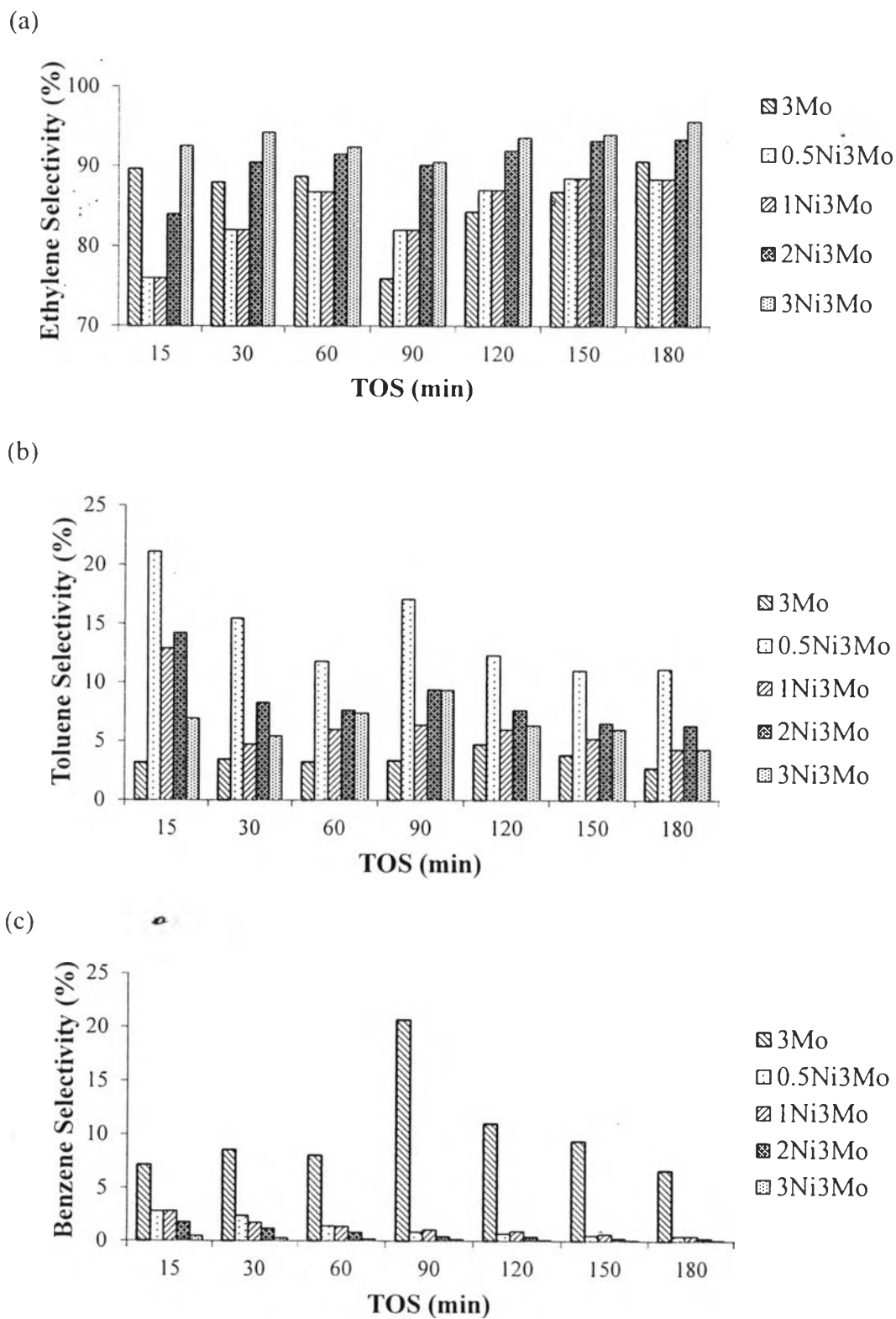


**Figure 4.11** Gaseous product selectivities for the unmodified Mo/HZSM-5 and modified by various Ni loadings (a) ethylene selectivity (b) toluene selectivity (c) benzene selectivity.

Ethylene yields on the modified catalysts are shown in Table 4.6. The bimetallic catalyst shows the ethylene higher than monometallic. The addition Ni onto 3%Mo/HZSM-5 can enhance the ethylene yield. Moreover, ethylene yields were increased with increasing of Ni loading. However, only 2%Ni-3%Mo/HZSM-5, the ethylene was dropped due to the high of coke formation that was shown in Table 4.7. From the table, among the catalysts tested, the 3%Ni-3%Mo/HZSM-5 provides the highest ethylene yield with which its syncline appears at a TOS of 90 min. It is postulated that the methane conversion into ethylene would be the primary reaction which takes place on the metal sites. Subsequently, the aromatization of ethylene to aromatics taking place on the Brønsted acid sites would be the secondary reaction. In the initial period of the reaction, the Brønsted acid sites were not covered or blocked by the deposited coke, and ethylene could easily be converted into aromatics resulting in decreasing the ethylene selectivity. As the reactions proceed, the Brønsted acid sites were deactivated by coke formation and/or the inaccessibility due to the pore blocking resulting in the increased ethylene selectivity.

**Table 4.6** Yield profiles of ethylene formation for the prepared catalysts

Catalyst	Yield of Ethylene (%) at TOS (min)						
	15	30	60	90	120	150	180
3%Mo/HZSM-5	0.29	0.21	0.29	0.24	0.17	0.19	0.28
3%Ni/HZSM-5	0.80	0.79	0.70	0.69	0.71	0.71	0.70
0.5%Ni-3%Mo/HZSM-5	0.42	0.29	0.47	0.39	0.46	0.51	0.51
1%Ni-3%Mo/HZSM-5	0.88	1.21	1.09	0.99	0.96	1.15	1.4
2%Ni-3%Mo/HZSM-5	0.78	0.70	0.91	0.70	0.88	1.10	1.05
3%Ni-3%Mo/HZSM-5	1.13	1.15	1.09	0.87	1.26	1.31	1.29



#### 4.2.2 Effect of Reaction Temperature

As the dehydrogenation coupling of methane is an endothermic reaction, high temperature will be advantageous for this reaction especially, the temperature between 700 °C to 800 °C is required to enhance conversion of methane (Yagita *et al.*, 1996). The 3%Ni-3%Mo/HZSM-5 was tested to compare under the different reaction temperature because it provides the highest performance among the bimetallic catalyst. The result of methane conversion and products selectivity on the 3%Ni- 3%Mo/HZSM-5 catalyst shows in Figure 4.12 and Figure 4.13 respectively. In the initial period of reaction, the catalyst that tested under 800 °C has the methane conversion higher than 750 °C after that was decreased due to the coke formation. After 120 min TOS, the catalyst that tested under 750 °C has the methane conversion higher than 800 °C and was decreased also. The different temperature provides the different maximum point of methane conversion.

The selectivity of ethylene in the range of TOS between 15 and 60 minute at 800 °C has selectivity lower than 750 °C and trend to increase with the TOS increase. Selectivity of toluene at 750 °C exhibits lower than 800 °C at the initial period of TOS and the maximum point at 90 min TOS. After 90 min TOS, selectivity of toluene decreased with TOS increased. On the other hand, selectivity of toluene at 800 °C decreased with catalyst exposed on long TOS and had the maximum point at 15 min TOS. Selectivity of benzene decreased with the TOS increasing. The dehydrogenation of methane is an endothermic reaction that caused the methane at high temperature was converted into the product faster than low reaction temperature and was favored for the coke formation that caused the catalyst deactivated rapidly.

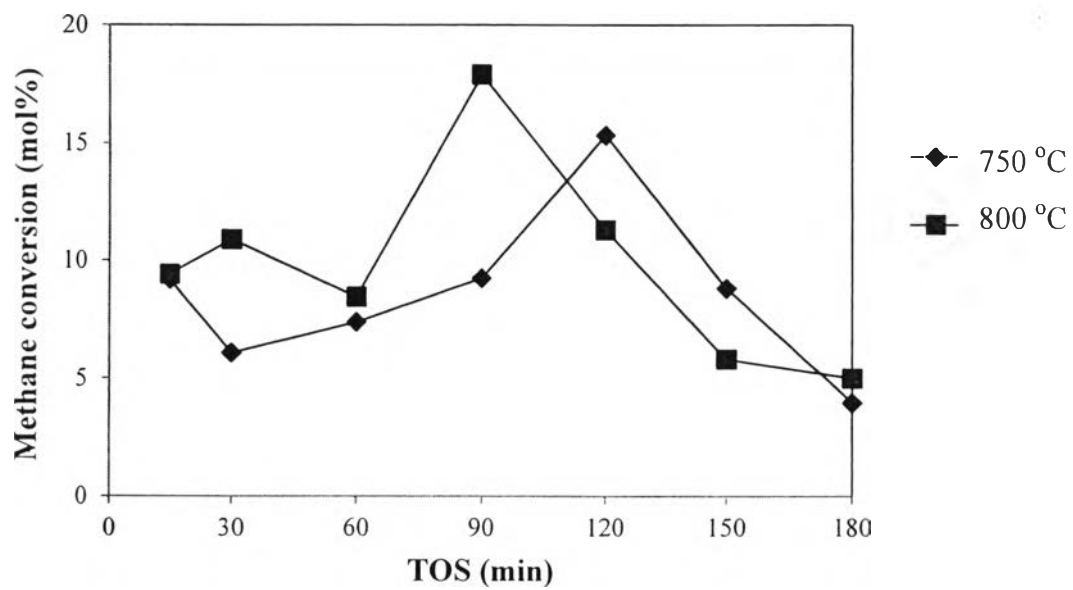


**Figure 4.12** Methane conversion over 3%Ni-3%Mo/HZSM-5 (750 °C and 800 °C, 20 % CH<sub>4</sub>, GHSV = 1,500 ml/g/h).

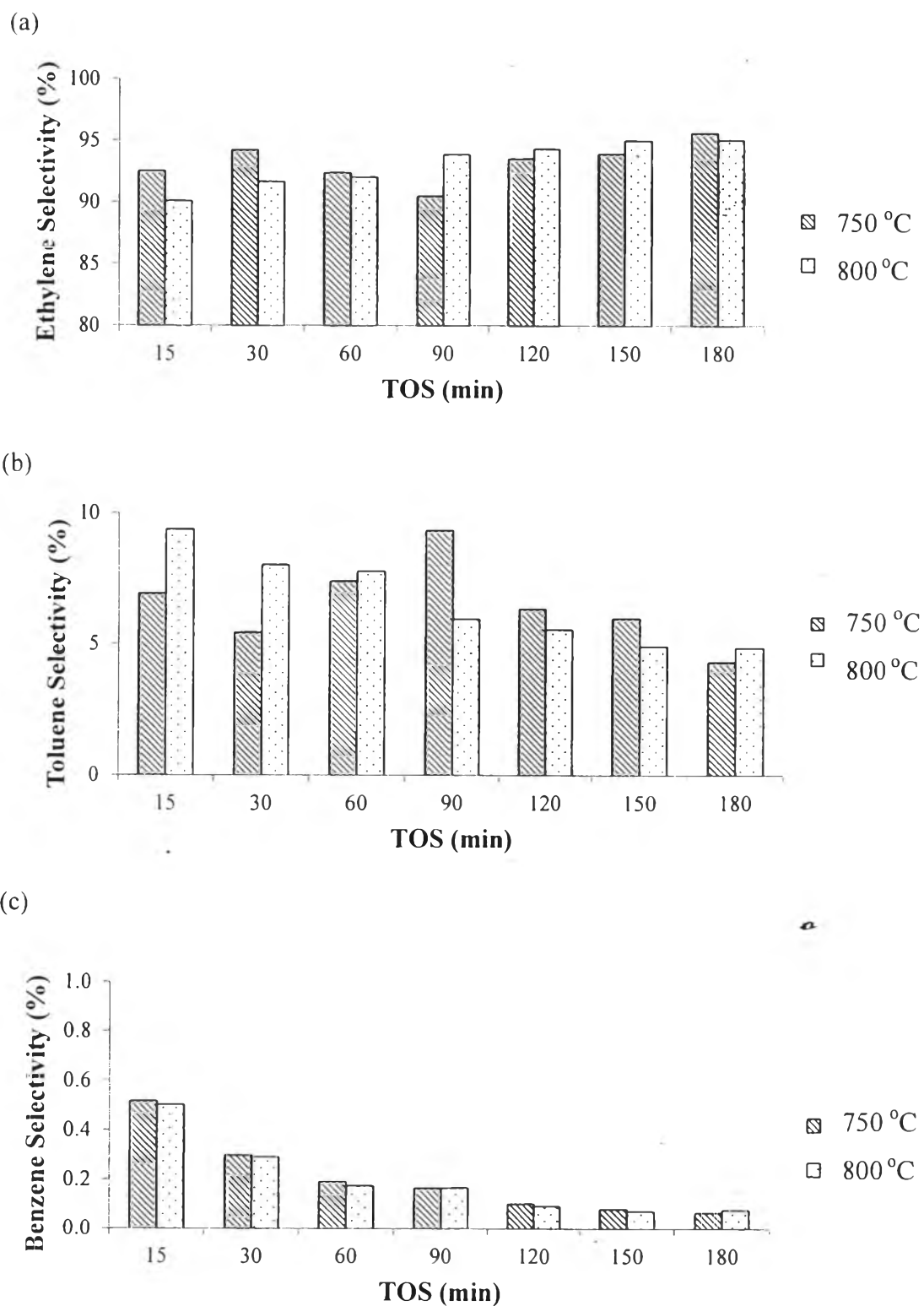


**Figure 4.13** Gaseous product selectivities for 3%Ni-3%Mo/HZSM-5 catalyst at different temperature reaction (a) ethylene selectivity (b) toluene selectivity (c) benzene selectivity.

#### 4.2.3 Effect of Methane Concentration

The change in methane concentration was carried out to study the catalytic performance for methane dehydrogenation and coupling to ethylene by varying methane in feed at 20 % and 40 % methane. The results of methane conversion and products selectivity on the 3%Ni- 3%Mo/HZSM-5 catalyst at various methane concentrations shows in Figure 4.14 and Figure 4.15 respectively.

In the initial period of reaction, the low methane feed concentration has the methane conversion higher than high concentration. After the 30 min TOS, the methane conversion was showed the opposite result, the high methane concentration provides the methane conversion higher than low concentration. According to the result of gaseous products selectivity as shown in Figure 4.15, the high methane concentration improves ethylene selectivity and reduces aromatics selectivity through course of reaction compared to low methane concentration. The high methane concentration provides the higher methane conversion and ethylene selectivity than low methane concentration. However, the catalyst was deactivated due to the coke formation on catalyst.

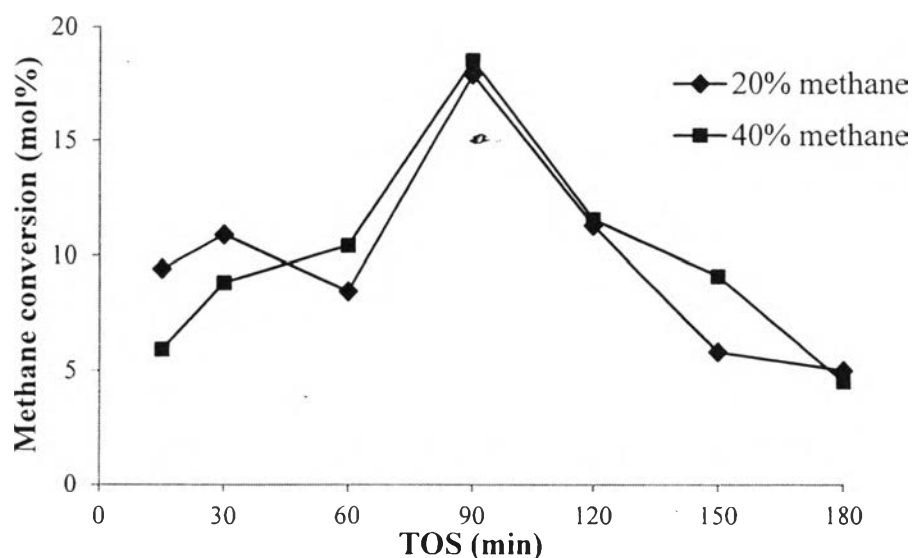


**Figure 4.14** Methane conversion over 3%Ni-3%Mo/HZSM-5 (800 °C, 20 % CH<sub>4</sub> and 40 % methane balanced in N<sub>2</sub>, GHSV = 1,500 ml/g/h).

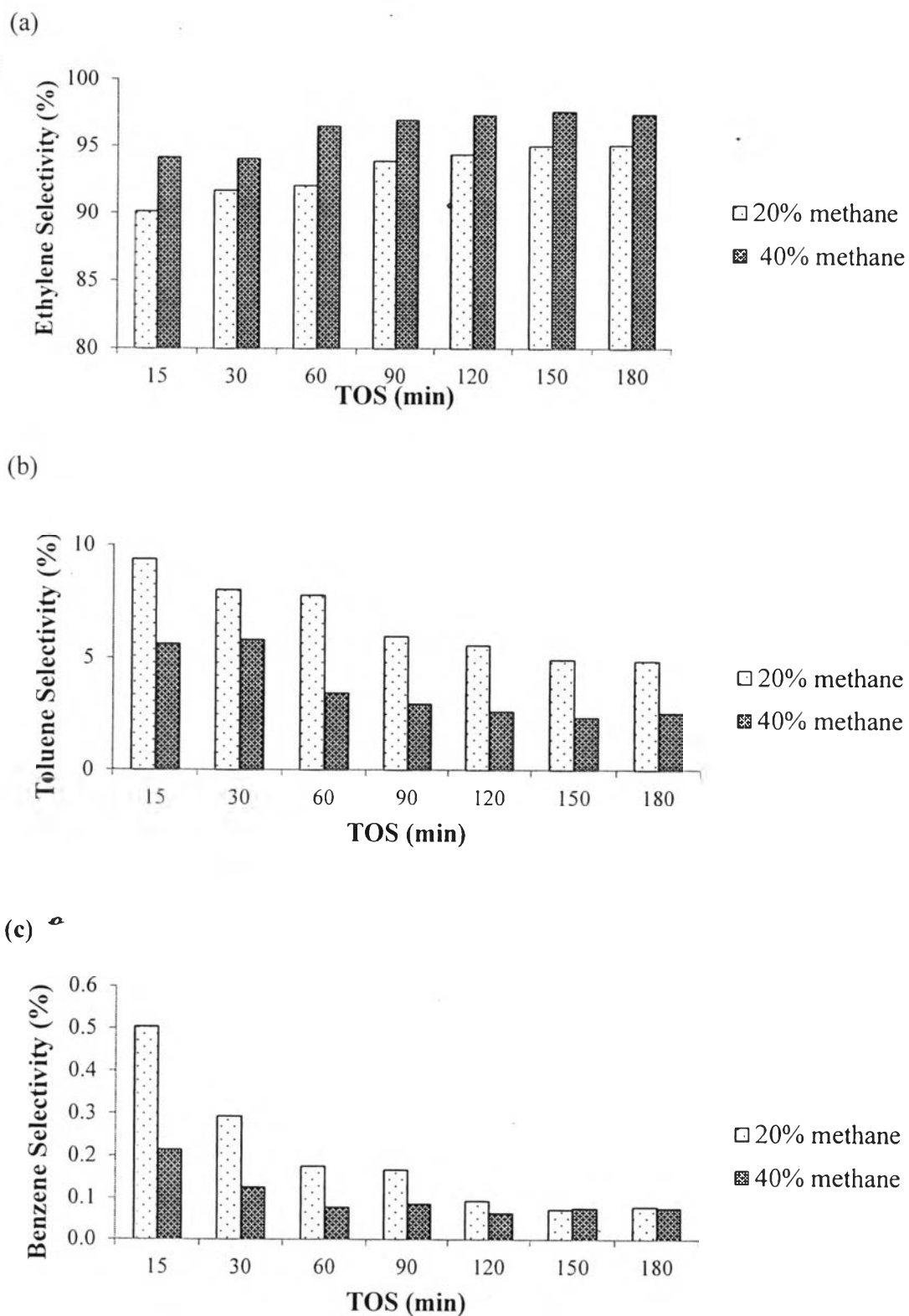


**Figure 4.15** Gaseous products selectivity over 3%Ni-3%Mo/HZSM-5 catalyst at different methane feed concentration and 800 °C (a) ethylene selectivity (b) aromatics selectivity (c) benzene selectivity.

#### 4.2.4 Coke Formation

The amount of coke deposited on catalysts was investigated by TPO technique. Table 4.7 presents coke formation on the spent catalysts under various reaction conditions. It can be observed that the overall catalysts that modified by addition of Ni had the amount of coke higher than 3%Mo/HZSM-5 and trended to increase with the Ni loading increased. However, 3%Ni-3%Mo/HZSM-5 provided the small amount of coke. It caused the highest activity that occurred on 3%Ni-3%Mo/HZSM-5.

The 3%Ni-3%Mo/HZSM-5 catalyst that was carried out at the low reaction temperature showed the coke formation lower than high reaction temperature. The high temperature generates 2 times of coke compare to low temperature. This can be suggested that high reaction temperature accelerated the deactivation of catalyst by high coke formation resulting in the methane conversion decreased rapidly. It can be suggested that high reaction temperature in feed accelerated the deactivation of catalyst.

The increasing of methane feed concentration has slightly affected for the coke formation. This result can observe in Table 4.7 that indicate the amount of coke over 3%Ni-3%Mo/HZSM-5 catalyst generates 2 times at reaction temperature of 800 °C

**Table 4.7** Coke formation on the spent catalysts.

Catalyst	Reaction Temperature (°C)	CH <sub>4</sub> Feed Concentration (mol%)	Amount of Coke (wt.%)
3%Mo/HZSM-5	750	20	0.99
3%Ni/HZSM-5	750	20	1.31
0.5%Ni-3%Mo/HZSM-5	750	20	1.06
1%Ni-3%Mo/HZSM-5	750	20	1.05
2%Ni-3%Mo/HZSM-5	750	20	1.76
3%Ni-3%Mo/HZSM-5	750	20	1.00
3%Ni-3%Mo/HZSM-5	800	20	2.08
3%Ni-3%Mo/HZSM-5	800	40	2.14